

Investigation on electromagnetically induced transparency and slowdown of group velocity in an $\text{Eu}^{3+}:\text{Y}_2\text{SiO}_5$ crystal

Qingchang LIANG¹, Haihua WANG², Zhankui JIANG (✉)^{1,2}

¹ Institute of Science and Technology for Opto-Electronic Information, Yantai 246005, China
² College of Physics, Jilin University, Changchun 130023, China

© Higher Education Press and Springer-Verlag 2008

Abstract Electromagnetically induced transparency (EIT) and slowdown of group velocity (SGV) in $\text{Eu}^{3+}:\text{Y}_2\text{SiO}_5$ were investigated by using density matrix equations of the interaction between light and matter and their numerical solutions. The relationship of the probe transmission with different probe detuning and coupling Rabi frequency was obtained. The influence of inhomogeneous line width on electromagnetically induced transparency and slowdown of group velocity were analyzed. Such transparency was restrained when inhomogeneous line width increased. The center transmission did not homogeneously change with an increase in ion-doped concentration. There is an optimal concentration which can make the electromagnetically induced transparency significant. It is evident that the group velocity of the probe has a minimum value for a certain level of coupling field strength.

Keywords quantum optics, quantum coherence effect, electromagnetically induced transparency (EIT), slowdown of group velocity (SGV), density matrix equation, $\text{Eu}^{3+}:\text{Y}_2\text{SiO}_5$

1 Introduction

During the last decade, physical phenomena based on quantum coherence effects such as electromagnetically induced transparency (EIT) [1–7], lasing without population inversion [8], slowdown of group velocity (SGV) [9], or nonlinear enhancement [10] were given much attention due to potential applications in optical information memory [11], optical computing [12], and nonlinear optics at low light levels [13,14]. However, most studies on quantum coherence phenomena are focused on atomic gas media, in which the applications are limited.

Translated and revised from *Acta Optica Sinica*, 2007, 27(5): 946–950 [译自: 光学学报]

E-mail: jzk@mail.jlu.edu.cn

Recently, one starts the investigation of quantum coherence effects in solid state materials [15]. Compared with gas media, these materials have advantages that include high atomic density, compact construction, and the absence of atomic diffusion, making development of devices easier. However, the essential difficulties in performing quantum coherence effects in solid state are wide optical linewidth and fast coherent decay time.

Ham et al. observed EIT in $\text{Pr}^{3+}:\text{Y}_2\text{SiO}_5$ crystal [15] and used the repumping method to reduce inhomogeneous linewidth in the optical transition. Turukhin et al. in 2002 reported ultraslow group velocity down to 45 m/s in the same crystal [16]. The general theory of quantum coherence effects in solids was given by Kuznetsova et al. [17].

In this paper, we analyzed EIT and SGV phenomena in an $\text{Eu}^{3+}:\text{Y}_2\text{SiO}_5$ crystal by using the semiclassical theory of the interaction between light and medium and discussed the influence of coupling field intensity, laser linewidth, inhomogeneous broadening, and ion-doped concentration on EIT and SGV. The aim of the paper is to establish the best experimental conditions for implementing EIT and SGV.

2 Theoretical model

The energy level system used in the theoretical model is shown in Fig. 1 as a Λ model. 7F_0 is the ground state of Eu^{3+} ion, which has three degenerate hyperfine levels ($\pm 1/2$, $\pm 3/2$, $\pm 5/2$), or the so-called spin sublevels; 5D_0 is an excited state of Eu^{3+} , which also has three hyperfine levels. ω_p , ω_c , ω_r are the frequencies of the probe field, strong coupling field and repumping field, respectively. The repumping light is used to avoid an empty population of the lower levels ($\pm 1/2$, $\pm 3/2$) due to ω_p , ω_c optical pumping. The repumping field does not enter the interaction density matrix. However, it has an influence on the inhomogeneous linewidth, i.e., the inhomogeneous linewidth of the optical transition is determined by the laser

linewidth. The interaction Hamiltonian for the Λ model of the three-level atomic system is

$$H_I = \hbar(\Delta_p - \Delta_c)|2\rangle\langle 2| + \hbar\Delta_p|3\rangle\langle 3| - (\hbar G_p|3\rangle\langle 1| + \hbar G_c|3\rangle\langle 2| + \text{H.C.}), \quad (1)$$

where 1, 2, 3 represent the three levels from high to low, respectively. Δ_p , Δ_c are the frequency detunings of the probe and coupling fields.

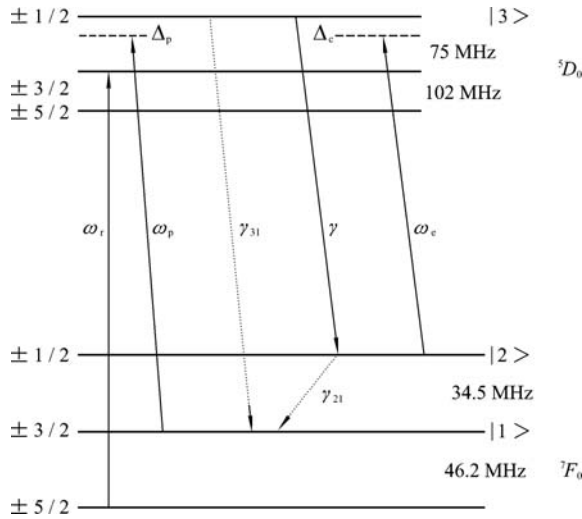


Fig. 1 Energy level diagram of $\text{Eu}^{3+}:\text{Y}_2\text{SiO}_5$

G_p and G_c are the Rabi frequencies of the probe and coupling fields defined by

$$G_p = \mu_{13}E_p/(2\hbar), \quad (2a)$$

$$G_c = \mu_{23}E_c/(2\hbar), \quad (2b)$$

where μ_{ij} is the dipolmoment between the i and j energy levels in the Eu^{3+} ion. E_p and E_c are the strengths of the probe and coupling fields. According to the theory of interaction density-matrix, given the population decay Γ and transition decay γ_{ij} , the dynamic equations for the density-matrix of the Λ model are determined by the principal equation

$$\frac{d\rho}{dt} = -\frac{i}{\hbar}[H, \rho] - \frac{1}{2}\{\Gamma, \rho\}, \quad (3)$$

which can be described by density-matrix elements as follows:

$$\dot{\rho}_{11} = \Gamma_{21}(\rho_{22} - \rho_{11}) + \Gamma_{31}\rho_{33} + iG_p(\rho_{31} - \rho_{13}), \quad (3a)$$

$$\dot{\rho}_{22} = -\Gamma_{21}\rho_{22} + \Gamma_{21}\rho_{11} + \Gamma_{32}\rho_{33} + iG_c(\rho_{32} - \rho_{23}), \quad (3b)$$

$$\dot{\rho}_{33} = -(\Gamma_{31} + \Gamma_{32})\rho_{33} + \Gamma_{31}\rho_{33} - iG_p(\rho_{31} - \rho_{13}) - iG_c(\rho_{32} - \rho_{23}), \quad (3c)$$

$$\dot{\rho}_{21} = [-\gamma_{21} + i(\Delta_p - \Delta_c + \Delta\omega_{21})]\rho_{21} - iG_p\rho_{23} + iG_c\rho_{31}, \quad (3d)$$

$$\dot{\rho}_{31} = [-\gamma_{31} + i(\Delta_p + \Delta\omega_{31})]\rho_{31} - iG_p(\rho_{33} - \rho_{11}) + iG_c\rho_{21}, \quad (3e)$$

$$\dot{\rho}_{32} = [-\gamma_{32} + i(\Delta_c + \Delta\omega_{31} - \Delta\omega_{21})]\rho_{21} - iG_p\rho_{23} + iG_c\rho_{31}, \quad (3f)$$

$$\dot{\rho}_{ij} = \dot{\rho}_{ji}, \quad (3g)$$

where $\Delta\omega_{31}$ and $\Delta\omega_{21}$ are the differences between the transition frequency of $|3\rangle$ to $|1\rangle$ and $|2\rangle$ to $|1\rangle$ with respect to the inhomogeneous line center. The first order of the approximate solution of ρ_{31} is

$$\rho_{31} = \frac{iG_p}{C} \frac{1}{2B} \left[-(\gamma_{21} + i\Delta_p - i\Delta_c + i\Delta\omega_{21})(4\gamma A\Gamma_{21} + 2G_c^2\gamma + \frac{G_c^2}{\gamma - i(\Delta\omega_{31} - \Delta\omega_{21} + \Delta_c)} 4\gamma A\Gamma_{21}) \right], \quad (4)$$

where

$$A = [\gamma^2 + (\Delta_c + \Delta\omega_{31} - \Delta\omega_{21})^2] / (2\gamma),$$

$$B = 4\gamma A\omega_{21} + \gamma G_c^2(1 + 3\Gamma_{21}/\Gamma_{32}),$$

and

$$C = (\gamma + i\Delta_p + i\Delta\omega_{31})(\gamma_{21} + i\Delta_e + i\Delta_c + i\Delta\omega_{21}) + G_c^2,$$

here $\gamma_{31} = \gamma_{32} = \gamma$ and $\Gamma_{12} = \Gamma_{21}$ have been assumed. ρ_{31} can be divided into imaginary and real parts, i.e.,

$$\rho_{31} = \chi' + i\chi'', \quad (5)$$

where χ' and χ'' represent the dispersion and absorption, respectively. Considering the inhomogeneous broadening W_{inh}^{ij} of the rare-earth ion in the crystal, the absorption of the probe field must be integrated with the linewidth,

$$\chi'' = \text{Im} \left[\iint f(\omega_{21})f(\omega_{31}) \frac{2N\mu_{31}\rho_{31}}{\epsilon_0 E_p} d(\omega_{31})d(\omega_{21}) \right], \quad (6)$$

where $\mu_{31}^2 = fe^2\hbar\lambda/(4\pi cm_e)$, e is electron charge, c is light velocity in vacuum, m_e is electron mass, and f is oscillator strength of the $|1\rangle \rightarrow |3\rangle$ transition,

$$f(\omega_{ij}) = W_{\text{inh}}^{ij} / \left\{ \pi \left[\Delta\omega_{ij}^2 - (W_{\text{inh}}^{ij})^2 \right] \right\},$$

as a function of the inhomogeneous line profile, which was assumed to be a Lorentzian function.

Table 1 Values of different parameters

γ^{-1}/ms	$\Gamma_{31}^{-1}/\text{ms}$	$\Gamma_{21}^{-1}/\text{h}$	$F/10^{-8}$	λ/nm	$\gamma_{21}^{-1}/\text{h}$	$W_{\text{inh}}^{21}/\text{kHz}$	N/cm^{-3}
477	2	24	1.2	578.879	2	100	1.8×10^{19}

Absorption coefficient

$$\alpha = K\chi'', \quad K = 2\pi/\lambda, \quad (7)$$

The transparency

$$T = \exp(-\alpha L), \quad (8)$$

where L is the sample length.

3 Numerical calculation of EIT

The transparency through the crystal can be calculated from Eqs. (4)–(8). The values of different parameters for $\text{Eu}^{3+}:\text{Y}_2\text{SiO}_5$, with 0.1% Eu^{3+} concentration, at temperature 1.4 K are given in Refs. [18–20] and listed in Table 1.

Inserting the parameters into Eqs. (4)–(8) and taking $L = 9 \text{ mm}$, $W_{\text{inh}}^{31} = 1 \text{ MHz}$ (laser linewidth), the transparency of the probe field as a function of detuning Δ_p was obtained, as shown in Fig. 2. Figure 3 shows the transparency at the center ($\Delta_p = 0$) as a function of G_c . It can be seen from Fig. 3 that the transparency increases as G_c increases rapidly at the region of G_c from 300 to 1000 kHz, and then increases slowly over 1000 kHz.

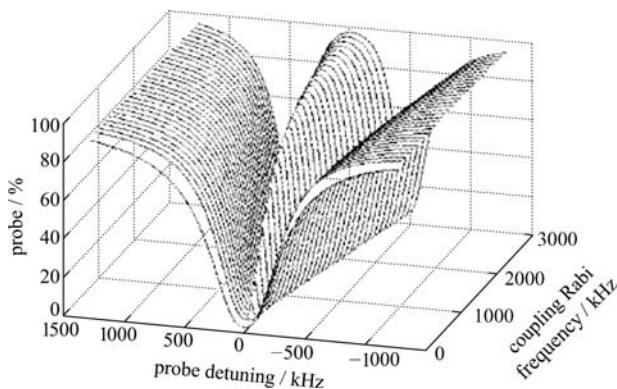


Fig. 2 Transmissivity of probe with different coherent fields and probe detuning

4 Influences of various parameters on EIT

4.1 Influence of inhomogeneous linewidth between spin sublevels on EIT

Keeping other parameters constant, changing only the inhomogeneous linewidth W_{inh}^{21} (0–100 kHz), and calculating the transparency as a function of W_{inh}^{21} , the results

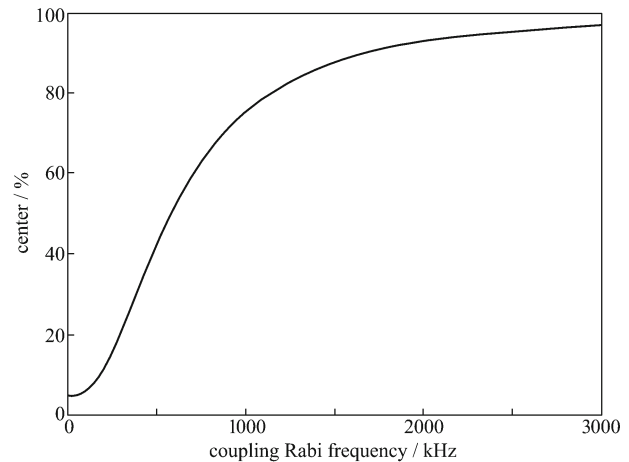


Fig. 3 Influence of coherent field intensity on center transmissivity

are shown in Fig. 4. Taking laser linewidth as 1 MHz and G_c as 500 kHz, it can be seen from the figure that transparency at the center decreases as W_{inh}^{21} increases.

4.2 Influence of inhomogeneous linewidth of optical transition on EIT

Keeping other parameters constant and changing only the inhomogeneous linewidth of the optical transition (i.e., laser linewidth in this model), the calculated results are shown in Fig. 5. In the calculations we took the values 100 kHz for the inhomogeneous linewidth of spin sublevel transition and 500 kHz for G_c . As shown in Fig. 5, the transparency at the center decreases gradually as the laser linewidth increases.

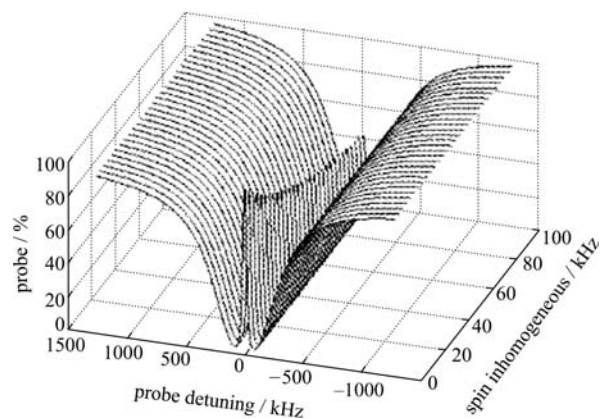


Fig. 4 Influence of inhomogeneous linewidth of spin sublevels on probe transmissivity

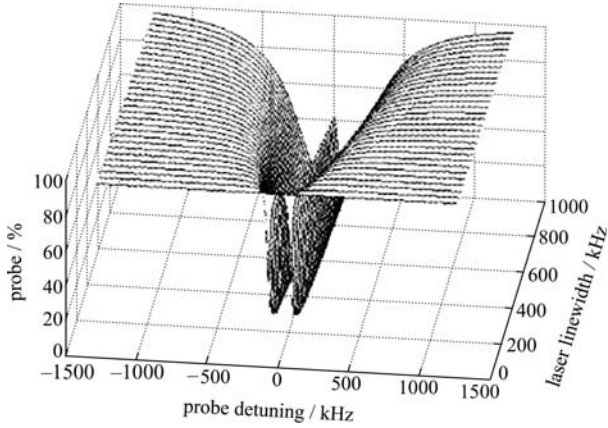


Fig. 5 Influence of optical inhomogeneous linewidth on probe transmissivity

4.3 Influence of Eu^{3+} ion-doped concentration on EIT

According to Ref. [20], the optical inhomogeneous broadening is related linearly with Eu^{3+} ion-doped concentration. Neglecting the effects of other factors, the influence of Eu^{3+} ion-doped concentration on the transparency of the probe field was obtained, as shown in Fig. 6. As can be seen from the figure, the transparency is not a simple function as the concentration, but it shows the best concentration for EIT.

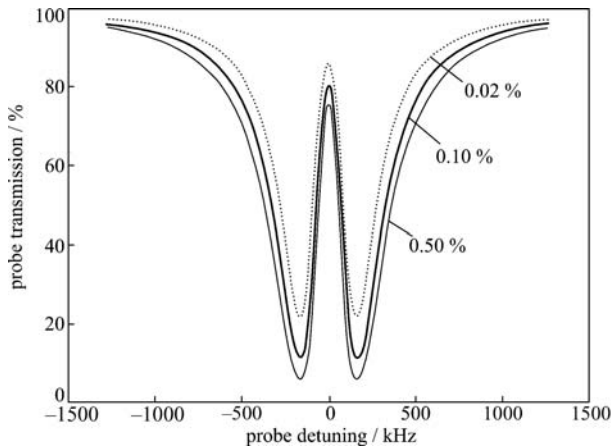


Fig. 6 Influence of different ion-doped concentrations on electromagnetically induced transparency

5 Preliminary investigation on SGV

In the region of the EIT, the medium refractive index will change rapidly, resulting in slowing group velocity that could even lead to stopping. The general expression for group velocity is

$$V_g = \frac{c}{n + 0.5v(d\chi'/dv)}, \quad (9)$$

where $n \approx 1 + 0.5\chi'$. Therefore, as soon as $d\chi'/dv$ is calculated, the group velocity will be obtained from Eq. (9). Using Eqs. (4)–(7), we calculated χ' as a function of probe detuning Δ_p and coupling Rabi frequency, as shown in Fig. 7. According to Eq. (9), when $\Delta_p = 0$ we calculated the group velocity V_g as a function of coupling intensity with different laser linewidths and the inhomogeneous linewidth of the spin sublevels, as shown in Figs. 8 and 9. It can be seen from Fig. 8 that before arriving at the minimum, V_g increases with the laser linewidth at the same coupling intensity, while the reverse case is revealed after the minimum. From Fig. 9 we can see that the minimum value of V_g decreases with a decrease of the linewidth of spin sublevels.

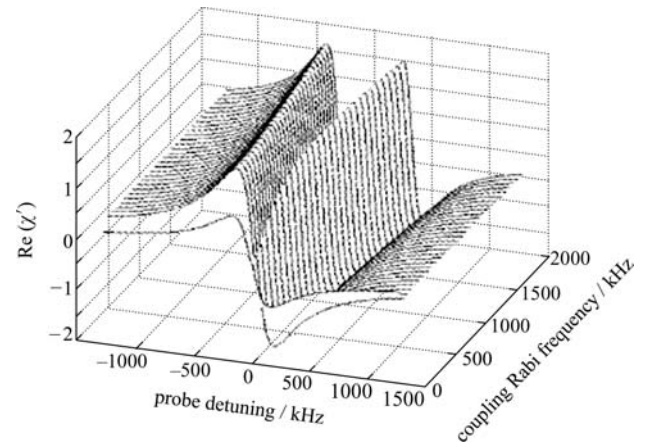


Fig. 7 Susceptibility χ' as a function of probe detuning Δ_p and coupling Rabi frequency

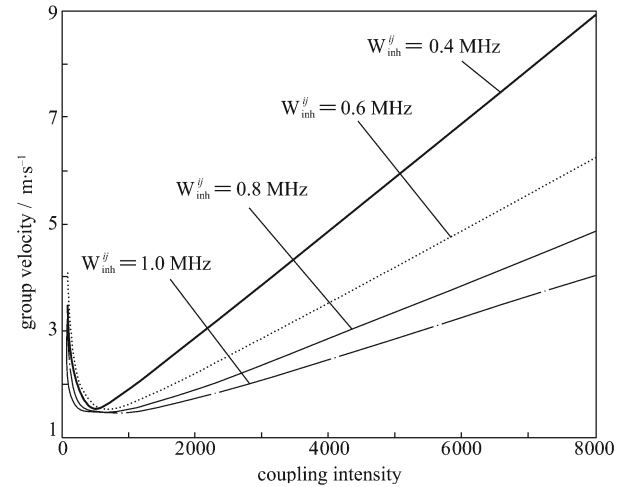


Fig. 8 Group velocity of different linewidths with different coupling intensities

6 Conclusion

In this paper, EIT and SGV in an $\text{Eu}^{3+}:\text{Y}_2\text{SiO}_5$ crystal were studied theoretically with a Λ model. The investiga-

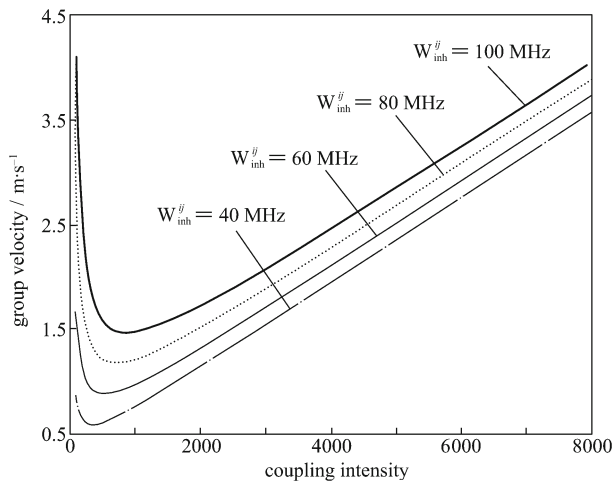


Fig. 9 Group velocity of different linewidths of spin sublevels with different coupling intensities

tion indicated that EIT evidently strengthened with an increase of the coupling field and was restrained by the laser linewidth and the inhomogeneous linewidth of the spin sublevels. Moreover, there is an optimal doped ion concentration which can make EIT significant. Calculation of the dependence of light group velocity on the coupling field showed that the group velocity has a minimum value for certain coupling fields. The influences of laser linewidth and inhomogeneous linewidth of the spin sublevels on group velocity were analyzed, showing that before arriving at the minimum, V_g increases as the laser linewidth increases at the same coupling intensity. The reverse case reveals that after the minimum, the minimum value of V_g decreases with a decrease of the linewidth of spin sublevels.

References

1. Xiao M, Li Y Q, Jin S Z, et al. Measurement of dispersive properties of electromagnetically induced transparency in rubidium atoms. *Physical Review Letters*, 1995, 74(5): 666–669
2. Gong S Q, Xu Z Z. Nonlinear theory of electromagnetically induced transparency. *Chinese Journal of Lasers*, 1996, 23(4): 311–314 (in Chinese)
3. Gong S Q, Xu Z Z, Zhang W Q, et al. Influence of driving field linewidth on electromagnetically induced transparency. *Acta Optica Sinica*, 1996, 16(3): 321–324 (in Chinese)
4. Boon J R, Zekou E, Fulton D J, et al. Experimental observation of a coherently induced transparency on a blue probe in a Doppler-broadened mismatched V-type system. *Physical Review A*, 1998, 57(2): 1323–1328
5. Yang S H, Guo X Z, Wang D, et al. Electromagnetically induced two-photon transparency and absorption enhancement. *Acta Optica Sinica*, 2000, 20(3): 309–314 (in Chinese)
6. Zhang Y L, Zhang X L, Sun Z R, et al. Double electromagnetically induced transparency and ultra-narrow line width in Y-type energy level system. *Acta Optica Sinica*, 2004, 24(4): 563–567 (in Chinese)
7. Dong Y B, Zhang J X, Gao J R. Quantum statistical property of radiation field in three-level electromagnetically induced transparency system. *Acta Optica Sinica*, 2005, 25(9): 1271–1276 (in Chinese)
8. Harris S E, Macklin J J. Lasers without inversion: single-atom transient response. *Physical Review A*, 1989, 40(7): 4135–4137
9. Harris S E. Pondermotive forces with slow light. *Physical Review Letters*, 2000, 85(19): 4032–4035
10. Harris S E. Lasers without inversion: interference of lifetime-broadened resonances. *Physical Review Letters*, 1989, 62(9): 1033–1036
11. Kocharovskaya O, Rostovtsev Y, Scully M O. Stopping light via hot atoms. *Physical Review Letters*, 2001, 86(4): 628–631
12. Fleischhauer M, Lukin M D. Dark-state polaritons in electromagnetically induced transparency. *Physical Review Letters*, 2000, 84(22): 5094–5097
13. Harris S E, Hau L V. Nonlinear optics at low light levels. *Physical Review Letters*, 1999, 82(23): 4611–4614
14. Lukin M D, Imamoglu A. Nonlinear optics and quantum entanglement of ultraslow single photons. *Physical Review Letters*, 2000, 84(7): 1419–1422
15. Ham B S, Hemmer P R, Shahriar M S. Efficient electromagnetically induced transparency in a rare-earth doped crystal. *Optics Communications*, 1997, 144(4–6): 227–230
16. Turukhin A V, Sudarshanam V S, Shahriar M S, et al. Observation of ultraslow and stored light pulses in a solid. *Physical Review Letters*, 2002, 88(2): 023602-1–023602-4
17. Kuznetsova E, Kocharovskaya O, Hemmer P, et al. Atomic interference phenomena in solids with a long-lived spin coherence. *Physical Review A*, 2002, 66(6): 063802-1–063802-13
18. Equall R W, Sun Y, Cone R L et al. Ultraslow optical dephasing in $\text{Eu}^{3+}:\text{Y}_2\text{SiO}_5$. *Physical Review Letters*, 1994, 72(14): 2179–2182
19. Longdell J J, Sellars M J, Manson N B. Demonstration of conditional quantum phase shift between ions in a solid. *Physical Review Letters*, 2004, 93(13): 130503-1–130503-4
20. Könz F, Sun Y, Thiel C W, et al. Temperature and concentration dependence of optical dephasing, spectral-hole lifetime, and anisotropic absorption in $\text{Eu}^{3+}:\text{Y}_2\text{SiO}_5$. *Physical Review B*, 2003, 68(8): 085109-1–085109-9